A novel micro-separator using the capillary separation effect with locally populated micro-pin-fin structure

Bin AN [1,*], Jinliang XU [1,2], Dongliang SUN [2]

* Jinliang Xu: Tel.: ++86 (10)61772268; Fax: ++86 (10)61772268; Email: xjl@nceou.edu.cn
1 State Key Laboratory of Alternate Electrical Power System with Renewable Energy Sources, North China Electric Power University, Beijing, 102206, China
2 Beijing Key Laboratory of Multiphase Flow and Heat Transfer, North China Electric Power University, Beijing, 102206, China

Abstract Phase separation is an important process in many chemical engineering applications, such as reactive processes and thermal separation processes of components. In this paper, a novel micro-separator was proposed using the capillary separation effect. The micro-pin-fins are locally populated in a rectangular microchannel, forming an enclosed region with micro pores as the boundaries. Hence, the microchannel cross section is divided into two symmetrical side regions closed to the microchannel side wall and a center enclosed region. When a two-phase stream interacts with the enclosed region boundary with micro-pores, the gas phase is prevented from entering the center enclosed region to enforce the gas phase flowing in the two side regions. Meanwhile, the liquid phase is flowing towards the center enclosed region. As a result, the two-phases are separated. The effect of the separator configuration parameters such as pin-fin size and distribution is also analyzed based on the computation results. The effect of phase separation is more obvious when the cross section area of side regions is decreased.

Keywords: Two Phase, Micro Flow, Phase Separation

1. Introduction

In the past decades, two-phase flows in the microchannel have been widely researched and applied in many fields, such as electronic micro-chips, capillary micro reactors, micro-electromechanical systems (MEMS) and heat exchangers to microscale assemblies. Compared to the traditional scale application, the advantages of microscale application show higher mass and heat transfer rates and surface-to-volume ratios (Aurux et al., 2002; Reyes et al., 2002; Hessel et al., 2009) Phase separation is an important process in many chemical engineering applications, such as reactive processes and thermal separation processes of components (Zhao and Middelberg, 2011). With the application of chemical engineering being more deeply, such as distillation and absorption, microstructure engineering becomes more and more important. The phase separation in micro assemblies should be further studied.

In order to achieve the stable phase separation, many different mechanisms are studied, such as centrifugal forces (Willems et al, 2008; Ma et al, 2009), gravity (Azzopardi, 1999; Das et al., 2005; Azzi et al., 2010; He et al., 2011)and surface tension forces (Adiche et al., 2010; David et al., 2011; Kraus and Krewer, 2011; Saad et al., 2011; Zenith et al., 2012). Especially, in the microscale field, the Laplace-length λ is an important parameter in phase separation which is defined as:

$$\lambda = \sqrt{\sigma / g(\rho_l - \rho_g)} \qquad (1)$$

where σ is the surface tension and ρ_l-ρ_g is the density difference between the liquid and gaseous phase. In conventional macroscale separator the size of the device is much larger than the Laplace length, then the surface tension is relatively less important (Aurux et al., 2002). On the contrary, the size of the separation device is smaller than Laplace length in micro system. Consquently, surface tension plays a dominant role in micro separators.

Several studies have dealt with phase separation using capillary forces. Changing the channel structure is an effective way to achieve phase separation. For example, Günther et al. (2004; 2005; 2006) presented a gas/liquid separator based on liquid-filled capillaries that achieve liquids separating from gas. The gas is prevented

from flowing into the capillary system, however, the addition pressure is imposed to force the liquid through the capillaries. On the other hand, surface modifications of microchannel walls with hydrophobic or hydrophilic is also a practicable method to achieve phase separation (Zhao et al., 2001; Hsieh and Yao, 2004; Hibara et al., 2005; Aota et al., 2007; Kraus and Krewer, 2011). Those methods are very effective due to exploiting interfacial tension and wetting, which are dominant effects in the microchannels. However, the modified walls can be damaged by heat and solvent properties of pH, which may make the phase separation failure.

To improve the above problem, in this paper, we proposed a phase separation model of gas-liquid two phase microflow in rectangular microchannel without additional drive force and the surface modification. The model is enlightened by Chen et al. (2012), who proposed a condenser to modulated flow patterns for enhancing condensation heat transfer at conventional scale. The micro-pin-fins are locally populated in a rectangular microchannel, forming an enclosed region with micro pores as the boundaries. The liquid phase and the gas phase went separated way. The performance of phase separation is generally investigated at the exact same operation condition using different separator parameters.

2. Simulation methods

2.1 Model geometry

Fig. 1 shows the structure of the micro-separator. A three-dimensional rectangular micro-channel with the length of 12 mm and cross-section area of 200×100 μm^2 was considered as the simulation case, inserted with a pin-fin with the cross-section area of 5×5μm^2 In the inlet section, the gas pumped by the main channel only goes perpendicular to the two liquid inlet channels. In the downstream of the channel, the micro-pin-fins were locally populated. As the reason that, for gas/liquid two-phase flow in a microchannel, the Taylor slug flow regime is the most commonly encountered flow pattern (Kreutzer et al., 2005), thus the present study deals with the numerical simulation of the Taylor flow in a micro-separator. The gas and liquid flow rates can be adjusted to produce Taylor slug flow. The gas and liquid inlet velocities are listed in Table 1, where both phases are laminar. The Taylor slug flow is modulated in the downstream direction where the micro-pin-fins are populated. The given parameters of the separators are summarized in Table 1.

Table 1
Geometry parameters of the microchannel (μm)

L	800	H	100
L_M	4000	w	5
L_B	8000	δ	5
D	200	--	--

2.2 Governing equations

A finite volume based commercial CFD package, FLUENT, was used to perform the numerical simulations. In order to track the

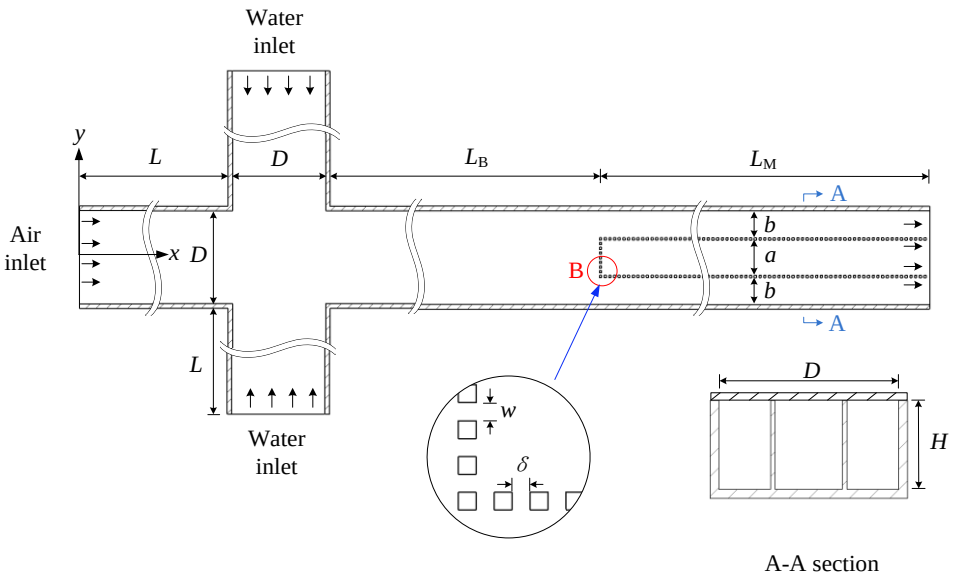

Fig. 1. The schematic diagram of microchannel structure

interface precisely between the gas and liquid, the volume of fluid (VOF) model (Hirt and Nichols, 1988) was adopted to simulate the two phase flow in the micro-separator. In micro-size channels, two-phase flow is dominated generally by the surface tension and the gravitational effects are relatively insignificant, thus, the gravitational effect is neglected in our study. The gas and liquid are assumed immiscible and phase unchangeable. The pressure drop along the separator is so small that the flow is treated as incompressible. The density of the water is ρ_L=998.2 kg/m^3 and of the air if ρ_G=1.225 kg/m^3 the surface tension is σ=0.0725 N/m . Under these assumptions, the fluid velocity field is given by the continuity equation:

$$\frac{\partial \rho}{\partial t} + \nabla \cdot (\rho \vec{v}) = 0 \qquad (2)$$

and the momentum equation,

$$\frac{\partial (\rho \vec{v})}{\partial t} + \nabla \cdot (\rho \vec{v} \vec{v}) = -\nabla p + \nabla \cdot \left[\mu \left(\nabla \vec{v} + \nabla \vec{v}^T \right) \right] + \vec{F}_{vol} \qquad (3)$$

where ρ and μ denote the density and the dynamic viscosity, respectively. The volume fraction of gas α_G is obtained by numerically solving Eq. (4), and the volume fraction of liquid α_L is simply computed from 1-α_G.

$$\frac{\partial \alpha_G}{\partial t} + \vec{v} \cdot \nabla \alpha_G = 0 \qquad (4)$$

$$\alpha_G + \alpha_L = 1 \qquad (5)$$

Both the density and viscosity are mixture properties, which vary within the flow domain and are computed by the volume fraction weighted average. Surface tension along the interface between the two phases becomes very important when the gravitational effect is negligible. The surface tension was modeled by the continuum surface force (CSF) model proposed by Brackbill et al. (1992) which is implemented in FLUENT. Thereby, the surface tension, represented as a volume force, is implemented in the momentum equation as a source term. It is given by Eq. (6).

$$\vec{F}_{vol} = \sigma \frac{\alpha_L \rho_L \kappa_L \nabla \alpha_L + \alpha_G \rho_G \kappa_G \nabla \alpha_G}{0.5(\rho_L + \rho_G)} \qquad (6)$$

where κ is the interface curvature having the following expression:

$$\kappa_L = \kappa_G = -\nabla \cdot \left(\frac{\nabla \alpha_L}{|\nabla \alpha_L|} \right) \qquad (7)$$

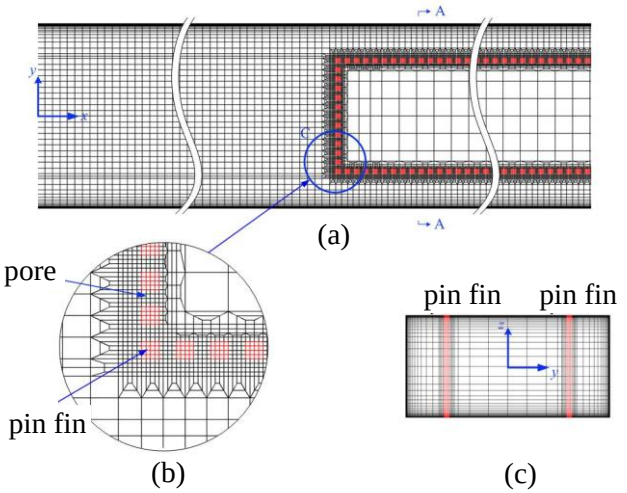

Fig. 2. The multi-scale grids for the microchannel. (a) top view; (b) local enlarged view of the region C ; (c) A-A cross section

2.3 Numerical approach

The cross section area of the channel is 200 μm×100 μm, while the micro-pin-fin area in the modulated section is 5 μm×5 μm. There is a large gap between the two parameters, hence the uniform scale grid would result in numerous number of grid. Consequently, different scales of mesh are implemented in the whole flow domain. The average grid sizes are 8 μm in the bare tube and 1.25 μm near the mesh pores. The different grid sizes are linked with each other by adapting the transition factor of 5:1. The grid size is 0.05 μm for the first layer of the tube wall as shown in Fig. 2.

A segregated time dependent unsteady solver was used. The boundary conditions were: velocity inlet for the gas and liquid feeds, specified as uniform entrance velocity, and pressure outlet at the exit. For discretization the Body Force Weighted scheme was employed for pressure interpolation, the SIMPLE scheme was used for pressure-velocity coupling, and the second-order upwind differencing scheme was used for the momentum equation. The Geometric Reconstruction method was employed for the resolution of the interface.

3. Result and discussion

3.1 Verification

In order to validate the numerical method, the two-phase frictional pressure drop in the bare section of the microchannel is compared with the correlation proposed by Kreutzer (2005), which is shown as follows:

$$\left(-\frac{dP}{dz} \right)_s = \frac{2\mu_f (u_f + u_g)}{D_h^2} \times 16 \left(1 + 0.07 \frac{D_h}{L_s} \left(\frac{\mathrm{Re}_{gl}}{Ca_{gl}} \right)^{0.33} \right) \qquad (8)$$

The pressure drop per unit length in our simulation is 0.972 MPa, while the value obtained from the correlation is 1.013MPa. The pressure drop deviation in the bare section was about less than 5%, indicating that the numerical model and the solution method are feasible.

3.2 Phase separation principle

Single-phase gas or liquid can pass though the micro pore freely. Only liquid phase can flow into the core region when the gas/liquid mixture enters the modulated section, leaving the gas phase out of the core region. Under the effect of the surface tension, the gas phase could not invade the core region and thereby enters the side regions. Due to the pore blocked by the gas interface, liquids in the front of the core region are stationary. Chen et al. (2012) performed the surface energy analysis to explain the reason why bubbles are prevented from entering the core region.

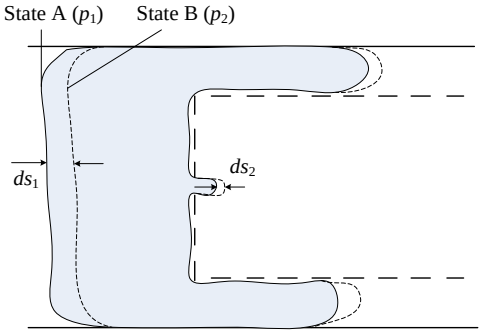

Fig. 3 The pressure difference analysis for a bubble penetrating over the pore

For the case with micro-pin-fins, when a large bubble is penetrating a rectangular pore, the surface energy of the gas bubble between states A and B is

$$dE = 2\sigma(w+H)ds_2 - 2\sigma(D+H)ds_1 \qquad (8)$$

where E is the surface energy, w is the pore width of the pins, D and H are the width and depth of the channel, respectively (see Fig. 3). The work required to transform the gas bubble from state A to state B is

$$dK = p_1 DHds_1 - p_2 Dwds_2 \qquad (9)$$

Therefore, the minimal pressure drop for bubble penetrating the pore is

$$p_1 - p_2 = 2\sigma\left(\frac{1}{w} - \frac{1}{D}\right) \qquad (10)$$

The second term on the right side of Eq. 10 gives less contributes as the reason of $D \geqslant w$. Given the parameters in our case, $p_1 - p_2$ = 28 KPa. This indicates that the pressure difference must be more than 28KPa to penetrate the pore. The smaller the width of the pore is, the much larger pressure difference is. The bubbles are prevented from flowing into the core region ensuring that the liquid phase can penetrate into the core region only.

3.2 Phase separation process

The contours of volume fraction for the micro-separator are illustrated in Fig. 4. Four characteristic features can be observed as follows: (1) Taylor flow was present in the bare section which exhibits as the periodic occurrence of the elongated bubbles. (2) When the bubble reached modulated region, the access to the core region for gas phase was prohibited by micro-pin-fin due to the surface tension. With the entire single bubble flowing into the side region, liquid slug starts to get though the core region until the next bubble coming. (3) Different from the initial shape of the bubble in the bare section, the bubble is squished by the walls and micro-pin-fin in the side region. (4) With more bubbles entering the side region, the liquid plug between bubbles is gradually squeezed to the core region, making the bubbles to merge together, thus, the liquid was separated from gas. The phase distribution over the cross section of the microchannel is also illustrated in Fig. 4(b). Fig. 5 shows the bubble shape and flow field in different sections. In the bare section, the bubble velocity is almost identical to the average velocity, and the slip ratio is approximately one. The bubble almost occupied the whole section in bare section, and yet the gas

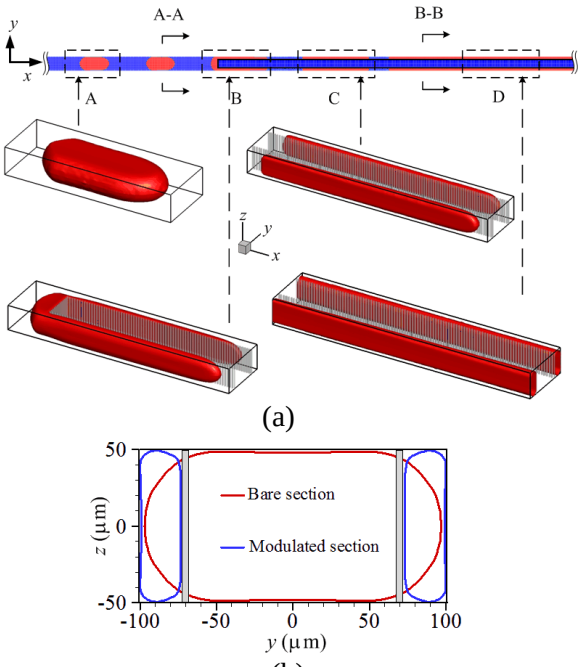

Fig. 4. Phase distribution in the microchannel for case 2, t = 21.6 ms

phase is discontinuous. As the mixture flowed in the modulated section, the mixture was separated into gas and liquid in different ways, in which the liquid phase took over the core region and the gas phase occupied the side regions, respectively. After the above process, the separation is achieved in the separator.

Although the micro-pin-fin prevented the entry of gas into the core region, the gas phase in the side region is still discontinuous. As seen in Fig. 4, the liquid plug length significantly decreased when compared with that of the gas slug, which indicated that the liquid in the side region was squeezed out. The main verification of the flow behavior is explained in Fig. 6, in which the pressure different between the side region and the core region is illustrated. When the bubble just reached the modulated section, the entrance of the core region along the flow direction was blocked by the bubble. Hence, the pressure drop along the core region is larger than that along the side region. A different pressure is present between the side region and the core region. As seen in Fig. 6, Δp was about 0.96 KPa when the liquid slug pass through the core region, on the contrary, when the gas pass through the core regions, it reached to 1.86 Pa. With the time increased during the "block" state, the pressure difference got progressively larger, even reached to 3.63 KPa as shown in Fig. 6(c). It would keep increasing until

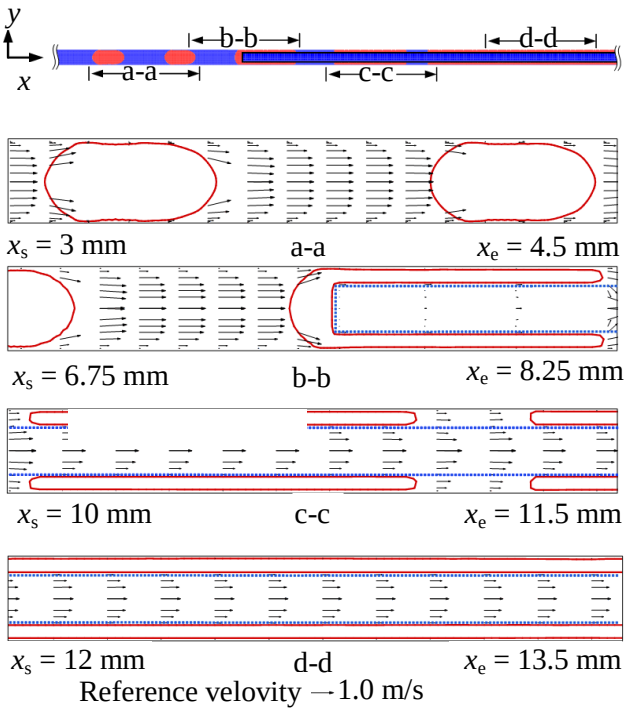

Fig. 5. Bubble shape and velocity field for case 2, t = 21.6 ms

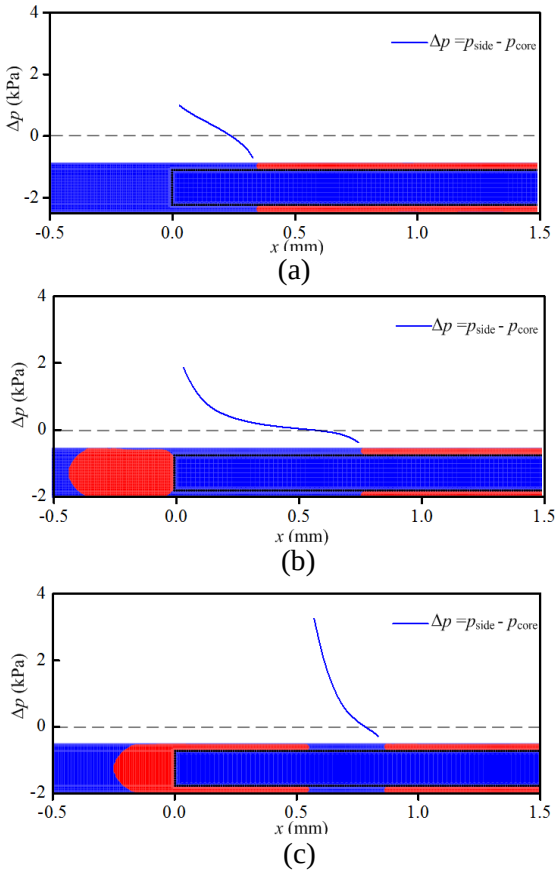

Fig. 6. Pressure differents between the side region and the core region (a) case 1, t =18.79 ms; (b) case 2, t =20.00 ms; (c) case 1, t = 19.48 ms

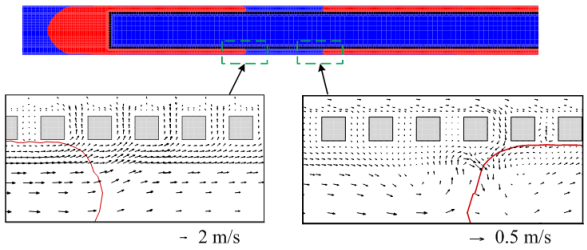

Fig.7 Near-pore-flow-field (case3, t = 19.49 ms)

the "block" in the entrance to the core region completely vanished. Liquids in the front of the core region are almost stationary as seen in Fig. 5(c).

The pressure difference will drive the mass transfer through the regions. The most significant pressure different occurs near the front of the bubble, associated with the change in the direction of the liquid flow as seen in Fig. 7(a). With the process of mass transfer, the pressure difference between the two regions would gradually decrease until the pressure balance reached. Fig. 7(a) depicts the flow field near the pore. It is obvious that the liquid plug in the side region was sucked into the core region through the pores between micro-pin-fins. The velocity of the liquid phase has the magnitude of 2 m/s.

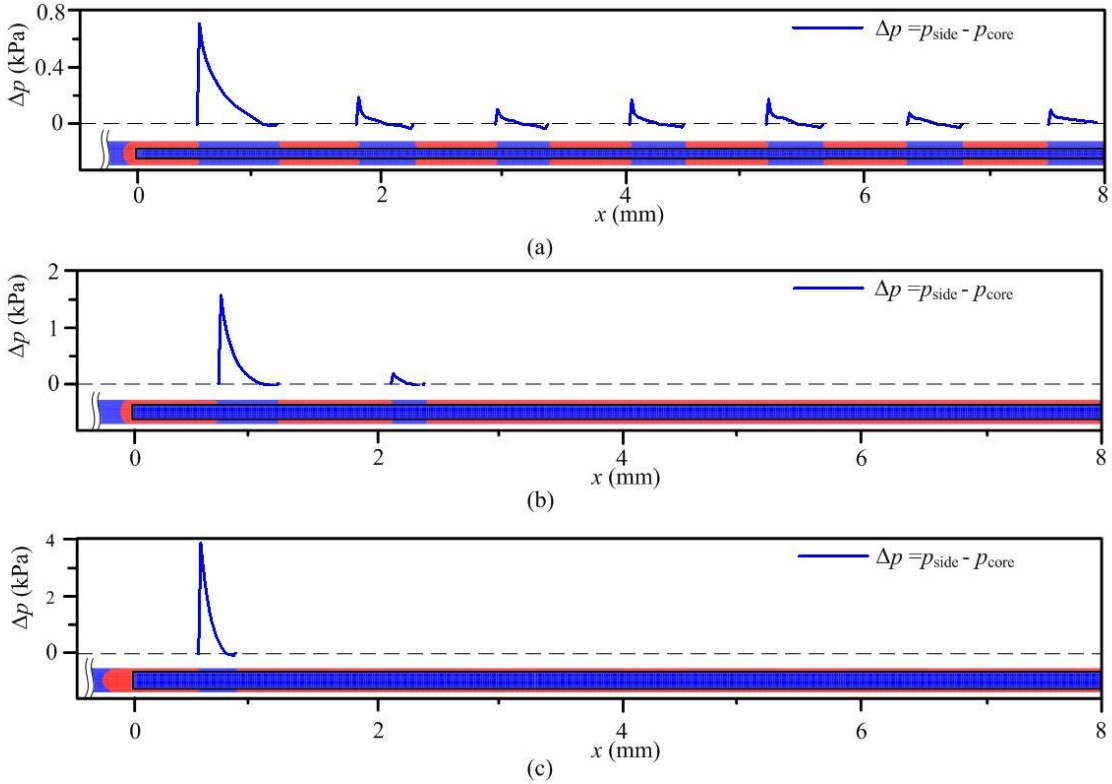

Fig. 8. Pressure differents between the side region and the core region (a) case 1, t =18.8 ms; (b) case 2, t =20.0 ms; (c) case 1, t = 19.5 ms t = 19.48 ms

Fig. 7(b) shows that there is some liquid at the nail of the bubble flow into the side region. This was reasonable since that there exists vortex inside the liquid slug between bubbles in Taylor flow. Considering that the gas was moving a little faster than the liquid, thus the space which bubble left be filled by the liquid film. In the side region, the liquid in the core region was sucked into the area because one side of walls consists of micro-pin-fin. The velocity magnitude at the tail of the bubble, which is about 0.5 m/s, is much less than that at the front of the bubble. Consequently, the liquid in the side region was squeezed out after taking into account the above competitive relation. Then the bubbles in the side region were completely merged as shown in region D (see Fig.(4)). Finally, separation is achieved in the micro-separator at the end of the channel by applying the micro-pin-fin in the microchannel.

3.4 Separation effect for different geometries

As stated above, the previous design is sufficient to remove liquid from the segmented gas-liquid flows. In this work, the separators with different micro-pin-fin arrangement have been investigated. The parameters of different separators are listed in Table 2. In order to analyze the influence of different structures on the phase separation, the same flow pattern of the two phase flow at the entrance of the separators is given. The result indicates that the distance between micro-pin-fin and the wall will influence the separation effectiveness.

Table 2.
Operating conditions for three different air-water slug flows.

Case	$u_{gas,in}$ (m/s)	$u_{liquid,in}$ (m/s)	Re_g	Re_l	a (μm)	b (μm)
1					80	60
2	0.1435	0.3345	1.228	50	120	40
3					140	30

As seen in Fig. 8, the flow pattern was changed after modulated in all the three cases. In the bare section, the length of the bubbles was slightly different for each case. This can be explained by the generation of the bubbles due to the different pressure distribution along the channel in each separator. Because the length difference for the three cases is small, so the generation of the Taylor flow is not the principal mechanisms of the separators investigated and this factor is neglect in this study.

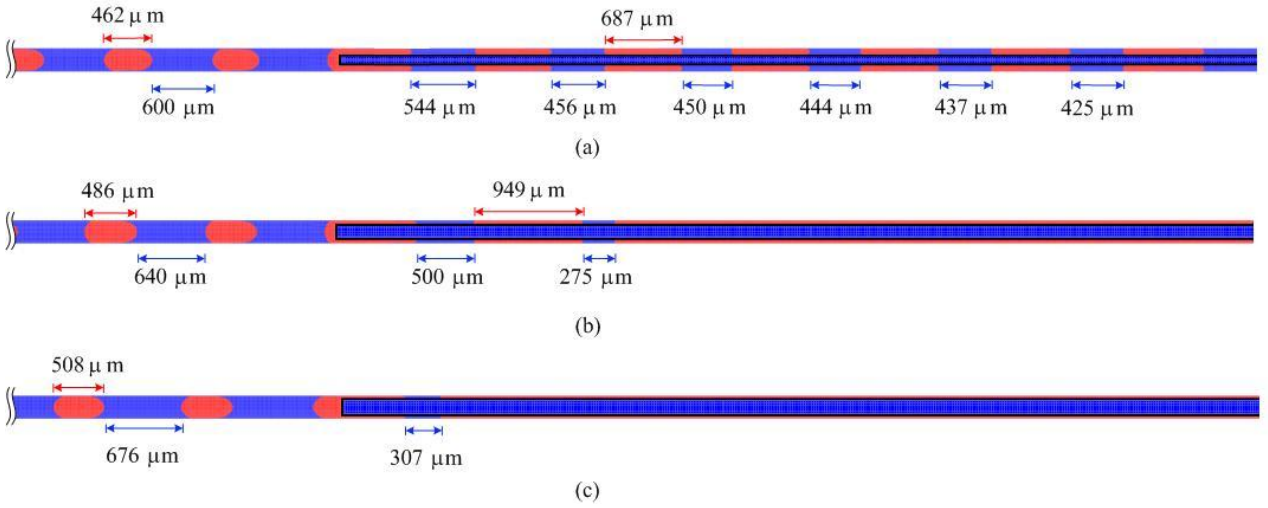

Fig. 9. Phase distribution in the microchannel at top view (a) case 1, t =18.8 ms; (b) case 2, t = 20.0 ms; (c) case 3, t = 19.5 ms

Phase separation was accomplished in case 2 and 3 except case 1. In case 1, the length of liquid plug in the side region was remarkably decreased from 600 μm to 450 μm, indicating that the liquid was actually flow from side to core region. The length of each liquid plug was decreased one by one along the flow direction. If all the liquid in the side region is expected to be squeezed out, a longer length of the channel is required. As mentioned above, for case 2 the bubble moved into the side region and was flatted out. Then the liquid between the bubbles were squeezed out until the bubbles merged together. In case 3, bubbles were already merged before they entirely flow into the side region. It is obviously that the efficiency was improved with the area of the core region flow section.

For all the three cases, the efficiency of the separator was different due to the fact that the pressure difference increased with the area of the core region flow section. This is evident comparing the value of the pressure difference in Fig. 9. Compared with the pressure difference in case 1, as the reason that the flow friction gets larger with the cross section area of the core region increased, the value in case 2 and 3 are much larger so that it could drive liquid squeezed out from the side region, resulting in the bubbles merged. Consequently, the capacity of the separator is governed by the arrangement of the micro-pin-fin. The smaller the distance is, the more apparent for the separator effectiveness is.

4. Conclusions

In this paper, a novel micro-separator was proposed using the capillary separation effect. The VOF method of computational fluid dynamics was used to investigate the phase separation in rectangular microchannel. From the studies of phase separation process and the influence of the separator structure, the following conclusions are drawn:

- The micro-pin-fin locally populated in the channel prohibited the gas to enter the core region and that ensure the core region is filled with pure liquid.
- The fact that liquid in the side region was sucked into the core region was caused by the pressure difference between the two regions, which is due to the fact that the gas blocked the entrance to the core region in flow section. Phase separation can be achieved with the liquid squeezed out from the side region.
- The arrangement of the micro-pin-fin has significant influence on the phase separation. The efficiency was improved markedly when the cross section area of the core region increased. As the cross section area increasing, the pressure different between the core region and the side region will rise. Once the pressure different beyond that caused by the surface tension, the gas would leak into the core region. Gas leaking phenomenon will be further studied in future work.
- Other influences on phase separation which will be studied on future works are: fluid properties and void fraction.

References

Adiche, C., Sundmacher, K., 2010. Experimental

investigation on a membrane distillation based micro-separator. Chem. Eng. Process. 49, 425–434.

Aota, A., Nonaka, M., Hibara, A., Kitamori, T., 2007. Countercurrent laminar microflow for highly efficient solvent extraction. Angew. Chem. Int. Ed. 46, 878

Auroux, P-A., Iossifids, D., Reyes, D.R., Manz, A., 2002. Micro total analysis systems. 1. Analytical standard operations and applications. Anal. Chem. 74, 2637.

Azzi, A., Al-Attiyah, A., Qi, L., Cheema, W., Azzopardi, B.J., 2010. Gas–liquid twophase flow division at a micro-T-junction. Chem. Eng. Sci. 65, 3986–3993.

Azzopardi, B.J., 1999. Phase separation at T-junctions. Multiphase Sci. Technol. 11, 223–329.

Brackbill, J.U., Kothe, D.B., Zemach, C., 1992. A continuum method for modeling surface tension. Journal of Computational Physics 100, 335–354.

Chen, H.X., Xu, J.L., Li, Z.J., Xing, F., Xie, J., Wang, W., Zhang, W., 2012. Flow pattern modulation in a horizontal tube by the passive phase separation concept. International Journal of Multiphase Flow 45, 12-23.

Das, G., Das, P.K., Azzopardi, B.J., 2005. The split of stratified gas–liquid flow at a small diameter T-junction. Int. J. Multiphase Flow 31, 514–528.

David, M.P., Miler, J., Steinbrenner, J.E., Yang, Y., Touzelbaev, M., Goodson, K.E., 2011. Hydraulic and thermal characteristics of a vapor venting two-phase microchannel heat exchanger. Int. J. Heat Mass Transfer 54, 5504–5516.

Günther, A., Khan, S.A., Thalmann, M., Trachsel, F., Schmidt, M.A., Jensen, K.F., 2004. Transport and reaction in microscale segmented gas–liquid flow. Lab Chip 4, 246–278.

Günther, A., Jhunjhunwala, M., Thalmann, M., Schmidt, M.A., Jensen, K.F., 2005. Micromixing of miscible liquids in segmented gas–liquid flow. Langmuir 21, 1547–1555.

Günther, A., Jensen, K.F., 2006. Multiphase microfluidics: from flow characteristics to chemical and materials synthesis. Lab Chip 6, 1487–1503.

He, K., Wang, S., Huang, J., 2011. The effect of flow pattern on split of two-phase flow through a micro-T-junction. Int. J. Heat Mass Transfer 54, 3587–3593.

Hessel, V., Renken, A., Schouten, J.C., Yoshida, J., 2009. Micro Process Engineering. A Comprehensive Handbook—Fundamentals, Operation and Catalysts, Wiley VCH, Weinheim, 1, 17–18.

Hibara, A., Iwayama, S., Matsuoka, S., Ueno, M., Kikutani, Y., Tokeshi, M., Kitamori, T., 2005. Surface modification method of microchannels for gas–liquid two phase flows in microchips. Anal. Chem. 77, 943–947.

Hirt C.W., Nichols, B.D., 1981, Volume of fluid (VOF) method for the dynamics of free boundaries, J. Comp. Phys. 39, 201–225.

Hsieh, C.-C., Yao, S.-C., 2004. Development of a microscale passive gas–liquid separation system. In: Proceedings of the 5th International Conference on Multiphase Flow. Yokohama, 30 May–4 June, p. 566.

Kraus, M., Krewer, U., 2011. Experimental analysis of the separation efficiency of an orientation independent gas/liquid membrane separator. Sep. Purif. Technol. 81, 347–356.

Ma, Q., Hu, D., He, G., Hu, S., Liu, W., Xu, Q., Wang, Y., 2009. Performance of innercore supersonic gas separation device with droplet enlargement method, separation science and engineering. Chin. J. Chem. Eng. 17, 925–933.

Kreutzer, M.T., Kapteijn, F., Moulijn, J.A., 2005. Inertial and Interfacial Effects on Pressure Drop of Taylor Flow in Capillaries. AIChE 51, 2427-2440.

Reyes, D.R., Iossifids, D., Auroux, P-A., Manz, A., 2002. Micro total analysis systems. 1. Introduction, theory, and technology. Anal. Chem. 74, 2623.

Saad, S.B., Clement, P., Gentric, C., Fourmigue, J.n.-F., Leclerc, J.-P., 2011. Experimental distribution of phases and pressure drop in a two-phase offset strip fin type compact heat exchanger. Int. J. Multiphase Flow 37, 576–584.

Willems, G.P., van Esch, B.P.M., Brouwers, J.J.H., Golombok, M., 2008. Creeping film model for condensed centrifugal separation processes. Chem. Eng. Sci. 63, 3358–3365.

Zhao, C.X., Middelberg, A.P.J., 2011. Two-phase microfluidic flows. Chem. Eng. Sci. 66, 1394–1411.

Zhao, B., Moore, J.S., Beebe, D.J., 2001, Surface-directed liquid flow inside microchannels. Science 291, 1023

Zenith, F., Kraus, M., Krewer, U., 2012. Model-based analysis of micro-separators for portable direct methanol fuel-cell systems. Comput. Chem. Eng. 38, 64–73.